Glucagon regulates gluconeogenesis through KAT2B- and WDR5-mediated epigenetic effects

Kim Ravnskjaer,[1] Meghan F. Hogan,[1] Denise Lackey,[2] Laszlo Tora,[3] Sharon Y.R. Dent,[4] Jerrold Olefsky,[2] and Marc Montminy[1]

[1]The Clayton Foundation Laboratories for Peptide Biology, The Salk Institute for Biological Studies, La Jolla, California, USA. [2]Department of Medicine, Division of Endocrinology and Metabolism, UCSD, La Jolla, California, USA. [3]Institut de Génétique et de Biologie Moléculaire et Cellulaire, CNRS UMR 7104, INSERM U964, Université de Strasbourg, Cedex, France. [4]Department of Molecular Carcinogenesis, Center for Cancer Epigenetics, MD Anderson Hospital, Smithville, Texas, USA.

Circulating pancreatic glucagon is increased during fasting and maintains glucose balance by stimulating hepatic gluconeogenesis. Glucagon triggering of the cAMP pathway upregulates the gluconeogenic program through the phosphorylation of cAMP response element–binding protein (CREB) and the dephosphorylation of the CREB coactivator CRTC2. Hormonal and nutrient signals are also thought to modulate gluconeogenic gene expression by promoting epigenetic changes that facilitate assembly of the transcriptional machinery. However, the nature of these modifications is unclear. Using mouse models and in vitro assays, we show that histone H3 acetylation at Lys 9 (H3K9Ac) was elevated over gluconeogenic genes and contributed to increased hepatic glucose production during fasting and in diabetes. Dephosphorylation of CRTC2 promoted increased H3K9Ac through recruitment of the lysine acetyltransferase 2B (KAT2B) and WD repeat–containing protein 5 (WDR5), a core subunit of histone methyltransferase (HMT) complexes. KAT2B and WDR5 stimulated the gluconeogenic program through a self-reinforcing cycle, whereby increases in H3K9Ac further potentiated CRTC2 occupancy at CREB binding sites. Depletion of KAT2B or WDR5 decreased gluconeogenic gene expression, consequently breaking the cycle. Administration of a small-molecule KAT2B antagonist lowered circulating blood glucose concentrations in insulin resistance, suggesting that this enzyme may be a useful target for diabetes treatment.

Introduction

In the fasted state, mammals shift from glucose to fat burning to maintain circulating glucose levels for glucose-dependent tissues. The liver provides glucose initially from glycogen stores and later through gluconeogenesis. During feeding, insulin inhibits the gluconeogenic program via the AKT-mediated phosphorylation of the forkhead domain protein FOXO1 (1); these effects are reversed during fasting, when decreases in insulin signaling promote FOXO1 dephosphorylation and activation.

Fasting also upregulates the gluconeogenic program through increases in circulating concentrations of pancreatic glucagon. Triggering of the cAMP pathway stimulates the protein kinase A–mediated phosphorylation of CREB, a modification that increases its association with the coactivator paralogs CBP and P300 (2). In parallel, glucagon also increases gluconeogenic gene expression via dephosphorylation and activation of the CREB-regulated transcriptional coactivator 2 (CRTC2; also referred to as TORC2) (3, 4). The gluconeogenic pathway is constitutively activated in insulin resistance, in which it promotes fasting hyperglycemia.

Under basal conditions, CRTC2 is highly phosphorylated and sequestered in the cytoplasm through phosphorylation at Ser171 by salt-inducible kinases (SIKs), members of the AMPK family of Ser/Thr kinases (5). Ser171 phosphorylation promotes 14-3-3 interactions that maintain CRTC2 in the cytoplasm. Exposure to glucagon stimulates CRTC2 dephosphorylation in part via the PKA-mediated phosphorylation and inhibition of SIKs (6). CRTC2 is also actively dephosphorylated by the calcium-dependent phosphatase calcineurin (7), which interacts directly with CRTC2. Following its dephosphorylation and nuclear translocation, CRTC2 associates with CREB over gluconeogenic promoters.

In addition to their effects on signal-dependent activators like CREB and FOXO1, hormone and nutrient signals are also thought to modulate gluconeogenic genes during fasting through epigenetic changes that facilitate assembly of the transcriptional machinery. These changes may become stabilized in diabetes, in which they contribute to pathological increases in circulating glucose levels. Here, we explore the role of histone-modifying complexes in mediating the induction of gluconeogenic genes during fasting and in diabetes. We found that, following their activation in response to glucagon, CREB and CRTC2 promoted the recruitment of lysine acetyl transferases (KATs) to gluconeogenic genes. In turn, these KATs promoted epigenetic changes that reinforced CREB/CRTC2 recruitment, particularly in insulin resistance, leading to the constitutive activation of the gluconeogenic program. Since the inhibition of relevant KAT activities in hepatocytes improved glucose homeostasis in diabetes, our studies point to these proteins as potential targets for therapeutic intervention.

Results

Hepatic KAT2B promotes H3K9 acetylation over gluconeogenic genes during fasting. We examined whether epigenetic changes contribute to hepatic glucose production by stimulating the gluconeogenic program during fasting and in diabetes. Amounts of hepatic

Conflict of interest: The authors have declared that no conflict of interest exists.
Citation for this article: *J Clin Invest.* 2013;123(10):4318–4328. doi:10.1172/JCI69035.

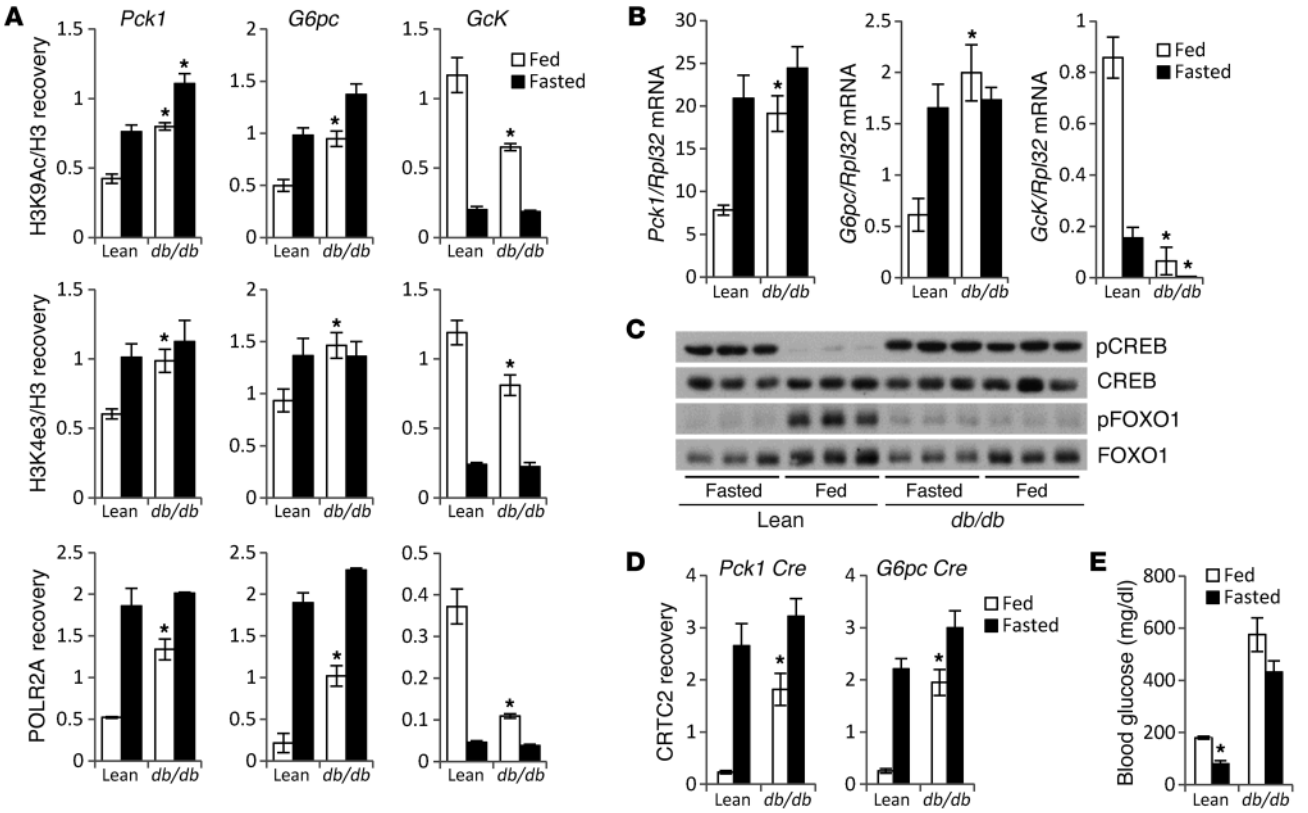

Figure 1

Increased H3K9 acetylation and H3K4 trimethylation over gluconeogenic genes in diabetes. (**A**) ChIP assay of histone H3 acetylated at K9 (H3K9Ac), histone H3 trimethylated at K4 (H3K4me3), and RNA polymerase II (POLR2A) over *Pck1*, *G6pc*, and *Gck* genes in livers from lean *db*/+ or diabetic *db*/*db* mice under fed and fasted conditions. H3K9Ac and H3K4me3 ChIP signals are normalized to total histone H3. (**B**) mRNA amounts for *Pck1*, *G6pc,* and *Gck*. (**C**) Immunoblot of pCREB and pFOXO1 protein amounts in livers from lean or *db*/*db* mice under fasted or fed conditions. (**D**) ChIP assay showing relative amounts of CRTC2 over CREB binding sites in *Pck1* and *G6pc* promoters in lean and *db*/*db* mice. (**E**) Twelve-hour fasting and fed blood glucose concentrations in lean and *db*/*db* mice. Error bars indicate the means ± SD (*$P < 0.05$ relative to lean mice; $n = 3–4$).

H3K9 acetylation (H3K9Ac) and histone H3K4 trimethylation (H3K4me3) — marks associated with active transcription — were low over the *Pck1* and *G6pc* genes in the fed state; they increased over these but not over housekeeping or feeding-inducible (*Gck*) genes during fasting, when CREB, FOXO1, and CRTC2 were active and when gluconeogenic gene expression was correspondingly high (Figure 1, A–C, and Supplemental Figure 1; supplemental material available online with this article; doi:10.1172/JCI69035DS1). By contrast, amounts of hepatic H3K9Ac and H3K4me3 over gluconeogenic genes were constitutively elevated in diabetes, paralleling the constitutive activation of CREB and FOXO1 and the increases in CRTC2 and RNA polymerase II occupancy (Figure 1, A–D). As a result, *Pck1* and *G6pc*, but not *Gck*, mRNA amounts were chronically upregulated in *db/db* mice relative to controls, leading to increases in circulating blood glucose concentrations (Figure 1E). In keeping with results from *db/db* mice, H3K9Ac amounts over *Pck1* and *G6pc* promoters were also constitutively elevated in high-fat diet–fed (HFD-fed) mice (Supplemental Figure 1A). In line with its role in active transcription, H3K36 trimethylation also increased over gluconeogenic genes during fasting and in diabetes (Supplemental Figure 1D). Not all histone marks were modulated by fasting or diabetes, however; H3K27 trimethylation and H3K27 acetylation appeared comparable under fasting and fed conditions and between wild-type and *db/db* mice.

H3K9 acetylation is catalyzed primarily by the KAT2 paralogs KAT2A (GCN5) and KAT2B (PCAF) (8, 9), while H3K4me3 amounts are modulated by histone methyltransferase (HMT) complexes that contain the core component WD repeat–containing protein 5 (WDR5) (10). We tested whether erasing these marks is sufficient to lower hepatic gluconeogenesis using adenovirally encoded RNAis to knock down relevant factors specifically in liver. Hepatic depletion of either *Kat2b* or *Wdr5* reduced gluconeogenic gene expression and circulating glucose concentrations after a 12-hour fast and had no effect on the feeding-dependent induction of *Gck* (Figure 2, A–C, and Supplemental Figure 2A). RNAi-mediated knockdown of *Wdr5* or *Kat2b* also downregulated gluconeogenic capacity in HFD-fed, insulin-resistant mice by pyruvate tolerance testing (Supplemental Figure 2B). In keeping with the reduction in glucose levels, we found that circulating glucagon concentrations were increased in *Wdr5*- and *Kat2b*-depleted mice relative to controls (Supplemental Figure 2C). In the liver, KAT2B appeared to be the predominant KAT2 isoform (11), with KAT2A protein being strongly upregulated upon *Kat2b* depletion (Supplemental Figure 2H and Supplemen-

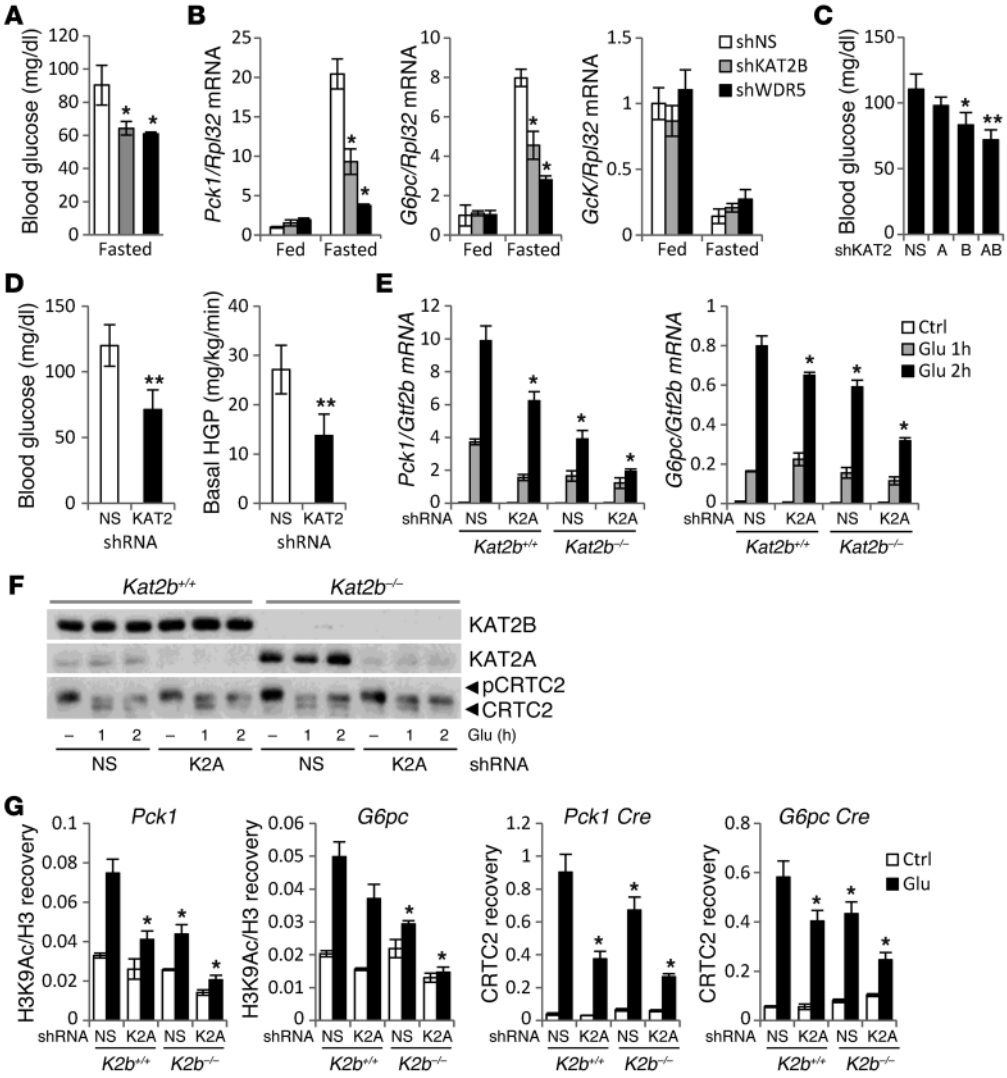

Figure 2
KAT2B promotes H3K9 acetylation and gluconeogenic gene expression. (**A** and **B**) Effects of hepatic knockdown of *Kat2b* and *Wdr5* with liver-specific adenovirally encoded RNAi on 12-hour fasting blood glucose (**A**) and mRNA amounts for *Pck1*, *G6pc*, and *Gck* genes (**B**) in 12-hour fasted and 2-hour refed mice. (**C**) Effect of hepatic *Kat2a* (denoted as A) and *Kat2b* (denoted as B) depletion alone or in combination on circulating glucose concentrations in 12-hour fasted mice. (**D**) Blood glucose and basal hepatic glucose production (HGP) after 6-hour fasting and effects of *Kat2a*/*b* depletion. (**E** and **F**) Effect of *Kat2a* depletion on gluconeogenic gene expression (**E**) and CRTC2 dephosphorylation (**F**) in hepatocytes from wild-type and *Kat2b*$^{-/-}$ mice. Exposure to glucagon is indicated. (**G**) ChIP assay of H3K9Ac and CRTC2 amounts over gluconeogenic genes in wild-type or *Kat2b*$^{-/-}$ hepatocytes depleted of *Kat2a*. Exposure to glucagon is indicated. CRTC2 and H3K9Ac ChIP signals were normalized to input and total histone H3, respectively (*P < 0.05; **P < 0.005 relative to NS RNAi; n = 4–5 and n = 3 for in vivo and in vitro experiments, respectively).

tal Figure 3C). Correspondingly, we observed that knockdown of both *Kat2a* and *Kat2b* had greater effects in reducing circulating glucose concentrations and gluconeogenic gene expression than either one alone, indicating some redundancy between these paralogs (Figure 2C and Supplemental Figure 3D). In line with their effects on gluconeogenic gene expression and on fasting glucose levels, hepatic depletion of KAT2A/B reduced basal hepatic glucose production in studies of fasted, lean C57Bl/6J mice with isotopically labeled glucose (Figure 2D).

Consistent with the effects of acute *Kat2b* knockdown, mice with a knockout of *Kat2b* also had lower fasting glucose levels and gluconeogenic gene expression relative to their wild-type littermates (Supplemental Figure 2, D–F). Despite the compensatory upregulation of KAT2A protein, the effect of KAT2B became penetrant under HFD conditions, when hepatic glucose production is typically upregulated. In keeping with their reduced blood glucose concentrations, we found that HFD-fed *Kat2b*$^{-/-}$ mice had elevated circulating glucagon levels and lower serum insulin concentrations relative to controls (Supplemental Figure 2, E and G). Taken together, these results indicate that hepatic KAT2B and WDR5 are required for hepatic glucose production during fasting.

KAT2B stimulates the gluconeogenic program in hepatocytes. We used *Kat2b*$^{-/-}$ hepatocytes to determine whether the effects of this coactivator on the gluconeogenic program are cell autonomous. In contrast with wild-type hepatocytes, glucagon increased the expression of gluconeogenic and other CREB target genes only modestly in *Kat2b*$^{-/-}$ cells (Figure 2E and Supplemental Figure 2I); RNAi-mediated knockdown of *Kat2a*, which is strongly upregulated in *Kat2b*$^{-/-}$ hepatocytes (Figure 2F), further reduced the expression of gluconeogenic genes in response to glucagon. Consistent with its effects on the gluconeogenic program, we observed that the depletion of *Kat2b* also reduced glucose secretion from primary hepatocytes (Supplemental Figure 2J). Arguing against an effect on the cAMP signaling pathway per se, exposure to glucagon triggered CRTC2 dephosphorylation comparably in wild-type versus *Kat2a*- and *Kat2b*-deficient hepatocytes (Figure 2F), yet loss of *Kat2a* and *Kat2b* reduced H3K9Ac amounts over both *G6pc* and *Pck1* genes (Figure 2G). As a result, CRTC2 recruitment to these promoters was correspondingly lower.

Based on the proposed role of H3K9 acetylation in stimulating the gluconeogenic program, we tested whether KAT2B catalytic activity is required for the induction of these genes in response to glucagon. *G6pc* and *Pck1* mRNA amounts were reduced in *Kat2b*$^{-/-}$

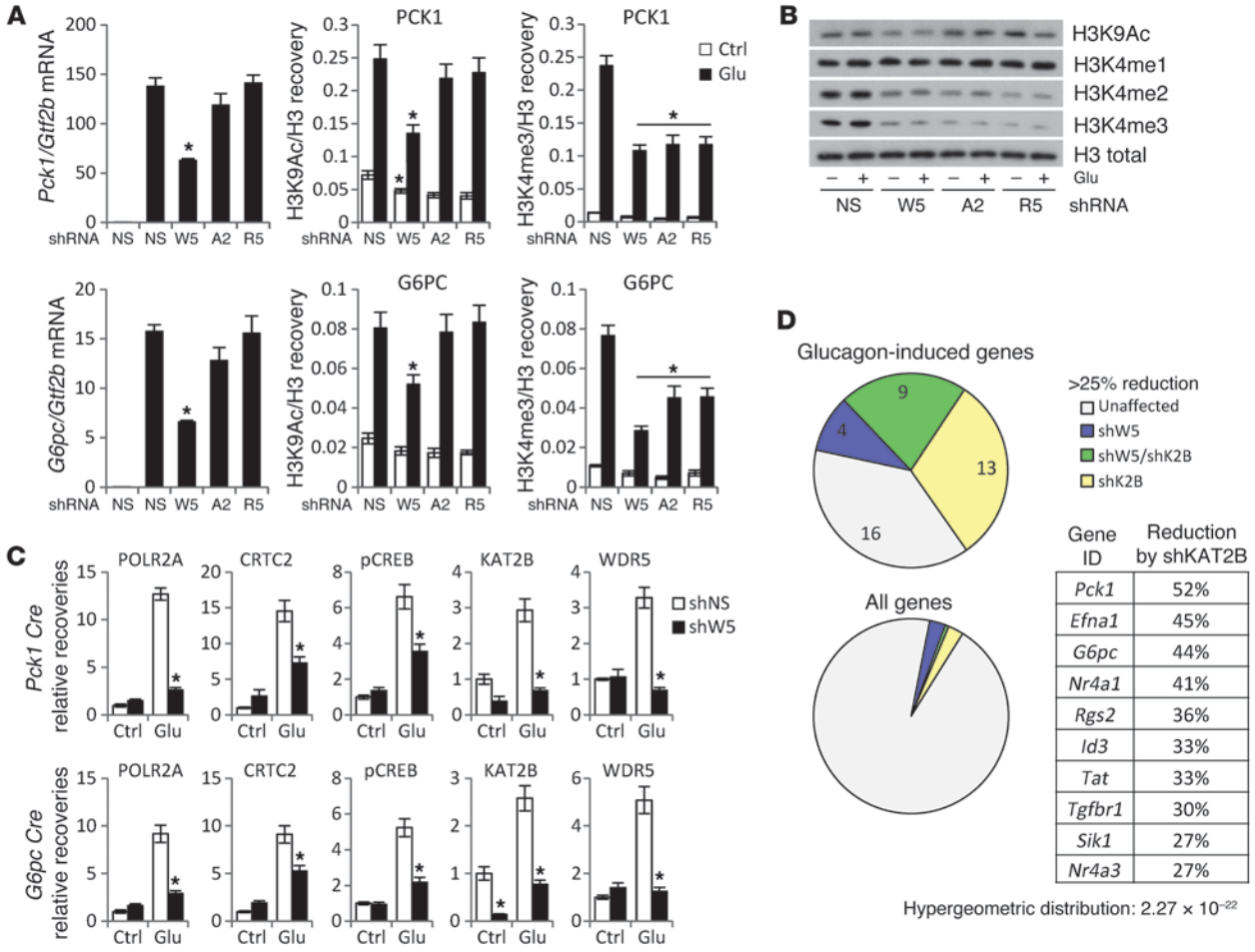

Figure 3

WDR5 promotes H3K9 acetylation and gluconeogenic gene expression through direct association with KAT2B. (**A**) Relative effects of *Wdr5* (W5), *Ash2l* (A2), and *Rbbp5* (R5) knockdown on gluconeogenic gene expression as well as H3K9Ac and H3K4me3 amounts over gluconeogenic genes in primary hepatocytes exposed to glucagon. H3K9Ac and H3K4me3 signals were normalized to total histone H3. (**B**) Immunoblot showing relative effects of *Wdr5*, *Ash2l*, and *Rbbp5* RNAis on H3K9 acetylation and H3K4 methylation in hepatocytes. (**C**) Effect of RNAi-mediated depletion of *Wdr5* on glucagon-induced recruitment of POLR2A, CRTC2, pCREB (Ser133), KAT2B, and WDR5 over CREB binding sites in the *Pck1* and *G6pc* promoters in hepatocytes (*$P < 0.05$ relative to NS RNAi; $n = 3$). (**D**) Microarray data showing fractions of all genes and glucagon-induced (>2-fold) genes that are reduced (>25%) by depletion of *Wdr5*, *Kat2b*, or by depletion of either *Wdr5* or *Kat2b* in hepatocytes (number of genes is indicated). List of glucagon-induced genes and their reduction upon *Kat2b* depletion. Hypergeometric distribution showing a strong overrepresentation of glucagon-induced genes among genes reduced by *Kat2b* depletion.

compared with wild-type hepatocytes exposed to glucagon, and the expression of wild-type KAT2B rescued both *G6pc* and *Pck1* gene expression (Supplemental Figure 2K).By contrast, we found that the expression of catalytically inactive (E551Q) KAT2B (12) did not restore gluconeogenic gene expression in *Kat2b*$^{-/-}$ cells, supporting an important role for KAT2B enzymatic activity.

KAT2A and KAT2B have been found to promote cellular gene expression in the context of large multisubunit complexes known as Spt-Ada-Gcn5 acetyltransferase (SAGA) (13, 14) or Ada two A containing (ATAC) (15–17). In ChIP assays of HEK293T cells, exposure to FSK triggered the recruitment of a SAGA (FAM48A), but not an ATAC-specific, subunit (ZZZ3) to CREB binding sites over the CREB target gene *Nr4a1* gene (Supplemental Figure 3A). Indeed, depletion of the SAGA component *Fam48a* reduced expression of the *G6pc* gene in hepatocytes exposed to glucagon, whereas knockdown of ATAC subunits (*Atac2*, *Yeats2*, or *Zzz3*) did not (Supplemental Figure 3B). Taken together, these results suggest that KAT2A and KAT2B are recruited to CREB binding sites as part of SAGA complexes, where they promote gluconeogenic gene expression in response to glucagon during fasting.

WDR5 promotes gluconeogenic gene expression in concert with KAT2B. We examined the effects of WDR5 in modulating the gluconeogenic program. Exposure to glucagon increased the amounts of H3K4me2 and H3K4me3 over *G6pc* and *Pck1*, but not over constitutively expressed genes in primary hepatocytes; these effects were blocked to a similar extent by depletion of *Wdr5* or other HMT core components (*Ash2l*, *Rbbp5*) (Figure 3A and Supplemental Figure 4). Surprisingly, knockdown of *Wdr5* decreased gluconeogenic gene expression, but depletion of *Ash2l* or *Rbbp5* did not. These results indicate that increases in H3K4me3, per se, may not be required for glucagon induction and that WDR5 must regulate this program via a different mechanism.

Supporting this idea, the depletion of *Wdr5* decreased H3K9Ac amounts over gluconeogenic genes as well as global H3K9Ac levels in hepatocytes, whereas the depletion of *Ash2l* or *Rbbp5* did not (Figure 3, A and B, and Supplemental Figure 4D). Based on these results, we tested whether WDR5 associates with and potentiates KAT2B activity over gluconeogenic genes. In co-IP studies, we recovered epitope-tagged WDR5 from IPs of both KAT2A and KAT2B (Supplemental Figure 5A). We found that WDR5 interacted with residues in KAT2B (aa 341–460) that are adjacent to the HAT domain in GST pulldown assays using purified WDR5 (Supplemental Figure 5B).

In view of its ability to associate with KAT2B, WDR5 may also enhance recruitment of KAT2B to gluconeogenic genes. Exposure to glucagon increased amounts of WDR5 and KAT2B over *G6pc* and *Pck1* promoters by ChIP assay (ref. 18 and Figure 3C). RNAi-mediated depletion of *Wdr5* disrupted KAT2B recruitment, leading to decreases in H3K9 acetylation over both genes (Figure 3C and Supplemental Figure 6A). Similar to *Kat2b* knockdown (Supplemental Figure 6, B and C), *Wdr5* depletion also reduced phospho-CREB (pCREB) and CRTC2 occupancy as well as RNA polymerase II recruitment to the *Pck1* and *G6pc* promoters in cells exposed to glucagon. Taken together, these results indicate that WDR5 contributes to gluconeogenic gene expression in part by enhancing *Kat2b* promotor occupancy and H3K9 acetylation in response to glucagon.

Despite their global effects on H3K9 acetylation, KAT2A and KAT2B appear to bind only a subset of cellular genes in genome-wide studies, suggesting that they may function more as gene-specific coactivators (15). In this study (15), CREB binding sites were enriched within the subset of KAT2A/B-occupied genes. In gene profiling studies of primary hepatocytes, knockdown of either *Kat2b* or *Wdr5* reduced the expression of only 6% of cellular genes (Figure 3D). By contrast, *Kat2b* or *Wdr5* depletion disproportionately decreased the expression of 60% of the glucagon-inducible genes, many of which contain CREB binding sites in their promoters. Gene Ontological (GO) analysis revealed that glucose and triglyceride metabolism were among the biological processes affected by *Kat2b* and *Wdr5* knockdown (Supplemental Table 2B). Indeed, *Pck1* and *G6pc* were among the top-scoring genes disrupted by *Kat2b* knockdown. These results support the idea that WDR5 and KAT2B modulate the gluconeogenic program in part through their effects on the CREB/CRTC2 pathway.

CRTC2 mediates recruitment of KAT2B to gluconeogenic promoters. Based on the ability of KAT2B to enhance CRTC2 recruitment to gluconeogenic promoters, we tested for an interaction between these proteins. We found that epitope-tagged CRTC2 associated with both KAT2A and KAT2B in response to the cAMP agonist (FSK) (Figure 4, A and B). The CRTC2-KAT2A/B interaction was constitutively increased in cells expressing phosphorylation-defective, and therefore nuclear (S171A), CRTC2 (Figure 4B). In mapping studies, KAT2B was found to recognize the carboxy-terminal acidic transactivation domain (TAD) (19) in CRTC2; a CRTC2 polypeptide lacking this 70–amino acid region (ΔTAD) did not associate detectably with KAT2B (Figure 4B). The interaction between CRTC2 and KAT2B appears direct; in GST pulldown assays, we recovered purified KAT2B from glutathione beads containing glutathionine S transferase (GST) CRTC2 (aa 601–692), but not GST alone (Supplemental Figure 7A).

Realizing that KAT2B associates with the CRTC2 TAD, we tested whether it correspondingly modulates CRTC2 transcriptional activity. In keeping with this idea, overexpression of KAT2A and KAT2B as well as WDR5 enhanced the activity of the TAD in the context of GAL4-CRTC2 fusion proteins containing the TAD, having no effect on a GAL4-CRTC2 ΔTAD polypeptide (Figure 4C and Supplemental Figure 7B).

The TAD is well conserved between CRTC family members, particularly at acidic residues (Figure 4D). Mutation of Glu665 and other acidic amino acids in the TAD disrupted its activity in transient assays (Supplemental Figure 7C). Pointing to a role for KAT2B in this process, mutation of E665 disrupted the CRTC2-KAT2B interaction by co-IP assay (Figure 4E). Moreover, overexpression of full-length E665K mutant CRTC2 had dominant-negative effects, reducing CREB reporter activity in HEK293T cells exposed to the cAMP agonist (Supplemental Figure 7D). By contrast, similar Lys substitutions at residues outside the TAD (E579, E587) did not alter CRTC2 activity relative to wild-type (Supplemental Figure 7D). In keeping with the results involving epitope-tagged and overexpressed proteins, we also found that endogenous KAT2B associated with endogenous CRTC2 in primary mouse hepatocytes following exposure to glucagon (Figure 4F).

If the recruitment of KAT2B to gluconeogenic promoters by CRTC2 is important for CREB target gene activation, then disrupting the KAT2B-CRTC2 interaction should reduce gluconeogenic gene expression in response to glucagon. We tested this idea in reconstitution assays using *Crtc2*$^{-/-}$ hepatocytes, in which KAT2B recruitment and gluconeogenic gene expression are downregulated. Adenoviral expression of wild-type CRTC2 fully restored KAT2B occupancy and H3K9Ac amounts over gluconeogenic genes in mutant cells exposed to glucagon, but the expression of KAT2B interaction–defective (E665K) CRTC2 did not (Figure 4, G and H, Supplemental Figure 7E, and Supplemental Figure 8, A–C). As a result, glucagon-dependent increases in RNA polymerase II recruitment and gluconeogenic gene expression were disrupted in E665K CRTC2–expressing cells, demonstrating the importance of CRTC2-KAT2B association for the locus-specific deposition of H3K9Ac marks and for induction of the gluconeogenic program in response to fasting signals.

Although knockout of CRTC2 reduced CREB target gene expression in hepatocytes, gluconeogenic gene expression was not completely downregulated in *Crtc2*$^{-/-}$ cells following exposure to glucagon. Based on the residual induction of these CREB target genes, we speculated that another CRTC family member may compensate in part for the loss of CRTC2. Supporting this idea, the CRTC2 paralog CRTC3 was readily detected in primary hepatocytes (Supplemental Figure 8E). In line with its ability to shuttle to the nucleus following its dephosphorylation in response to cAMP, exposure to glucagon also stimulated CRTC3 dephosphorylation and activation in primary hepatocytes (Supplemental Figure 8, E and H). Similar to CRTC2, we found that CRTC3 interacted with KAT2B in co-IP experiments with epitope-tagged CRTC3 (Supplemental Figure 8F). RNAi-mediated depletion of CRTC3 in hepatocytes reduced gluconeogenic gene expression and glucose output in wild-type hepatocytes and to a greater extent in *Crtc2*$^{-/-}$ or CRTC2 knockdown cells (Supplemental Figure 8, D, G, and I). Taken together, these results indicate that CRTC3 also regulates gluconeogenic genes and compensates in part for the loss of CRTC2 in hepatocytes.

Inhibition of KAT2B improves glucose balance in insulin-resistant mice. Because KAT2B and CRTC2 appear to exert mutually reinforcing effects on promoter occupancy, we considered that insulin resistance may trigger a feed-forward cycle of activation in which the CRTC2-dependent recruitment of KAT2B leads to increases in

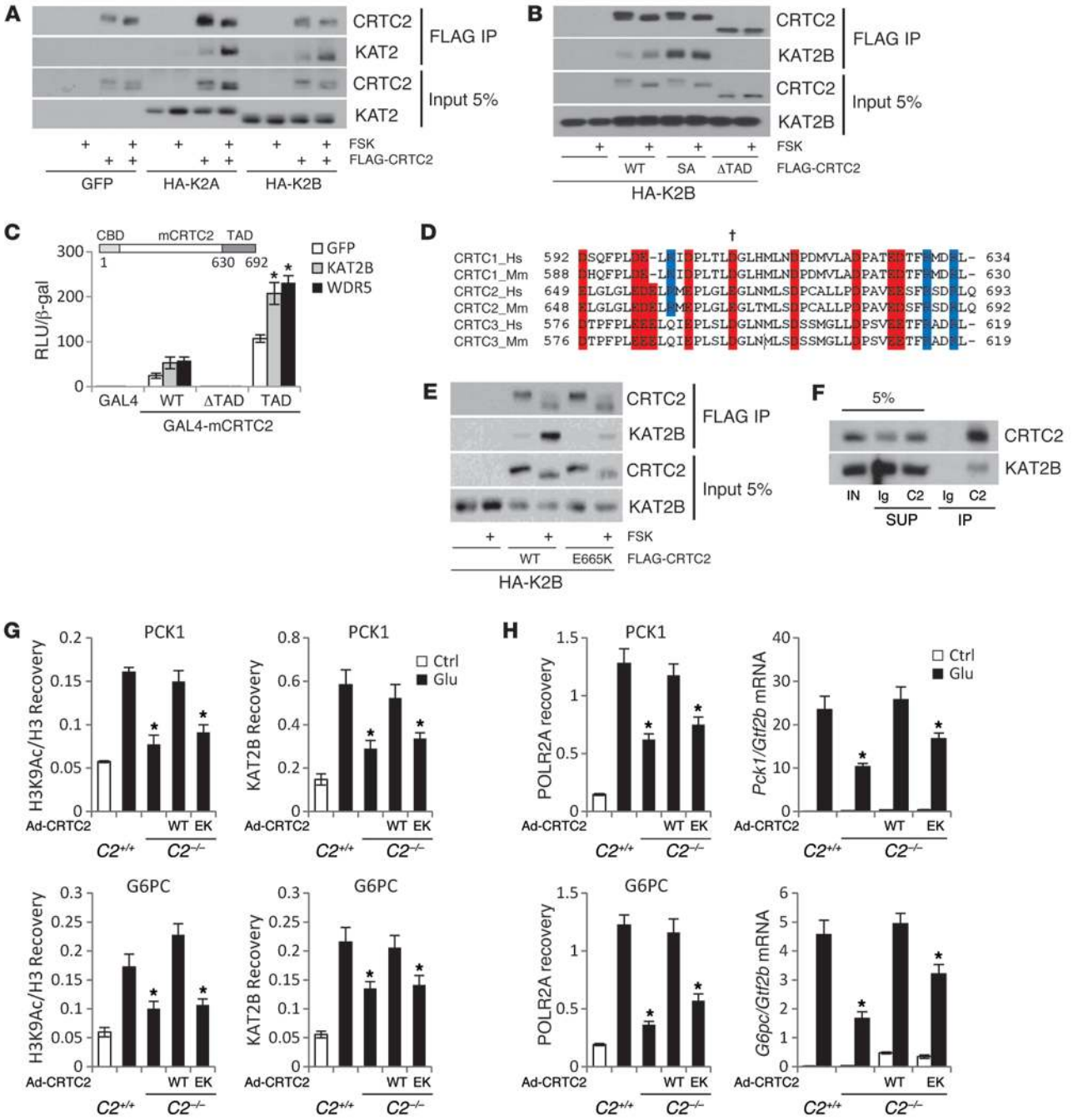

Figure 4

CRTC2 mediates the recruitment of KAT2B to promoters of gluconeogenic genes in response to glucagon. (**A** and **B**) Immunoblots showing amounts of HA-KAT2A and HA-KAT2B recovered from IPs of FLAG epitope–tagged wild-type (WT) CRTC2 (aa 1–692), phosphorylation–defective CRTC2 (SA, S171A), or CRTC2 ΔTAD lacking the TAD (aa 1–632) in HEK293T cells exposed to FSK for 1 hour. (**C**) Transient assay of chromosomal GAL4-Luc reporter activity in HEK293T cells expressing GAL4-CRTC2 constructs containing the GAL4 DNA-binding domain fused to wild-type CRTC2, CRTC2 ΔTAD, or to the TAD alone (aa 624–692). Effects of GFP, KAT2B, or WDR5 overexpression on GAL4 CRTC2 activity are shown. Luciferase activity was normalized to β-gal activity. (**D**) Alignment of TADs in mouse and human CRTC1, 2, and 3. Conserved acidic residues in red (†conserved Glu665, important for mCRTC2 interaction with KAT2B). (**E**) Immunoblot of HA-KAT2B amounts recovered from IPs of FLAG-tagged wild-type or E665K mutant CRTC2 prepared from HEK293T cells. One-hour treatment with FSK is indicated. (**F**) Immunoblot of endogenous CRTC2 and KAT2B co-IP from primary mouse hepatocytes exposed to glucagon for 1 hour. C2, CRTC2; Ig, IgG control; IN, input; SUP, supernatant. (**G** and **H**) Effect of glucagon on H3K9Ac amounts and KAT2B occupancy (**G**) as well as RNA polymerase II recruitment and mRNA amounts (**H**) for gluconeogenic genes in wild-type and *Crtc2*$^{-/-}$ hepatocytes reconstituted with wild-type or E665K (EK) mutant CRCT2. Exposure to glucagon for 90 minutes is indicated (*$P < 0.05$ relative to glucagon-stimulated *Crtc2*$^{+/+}$; $n = 3$).

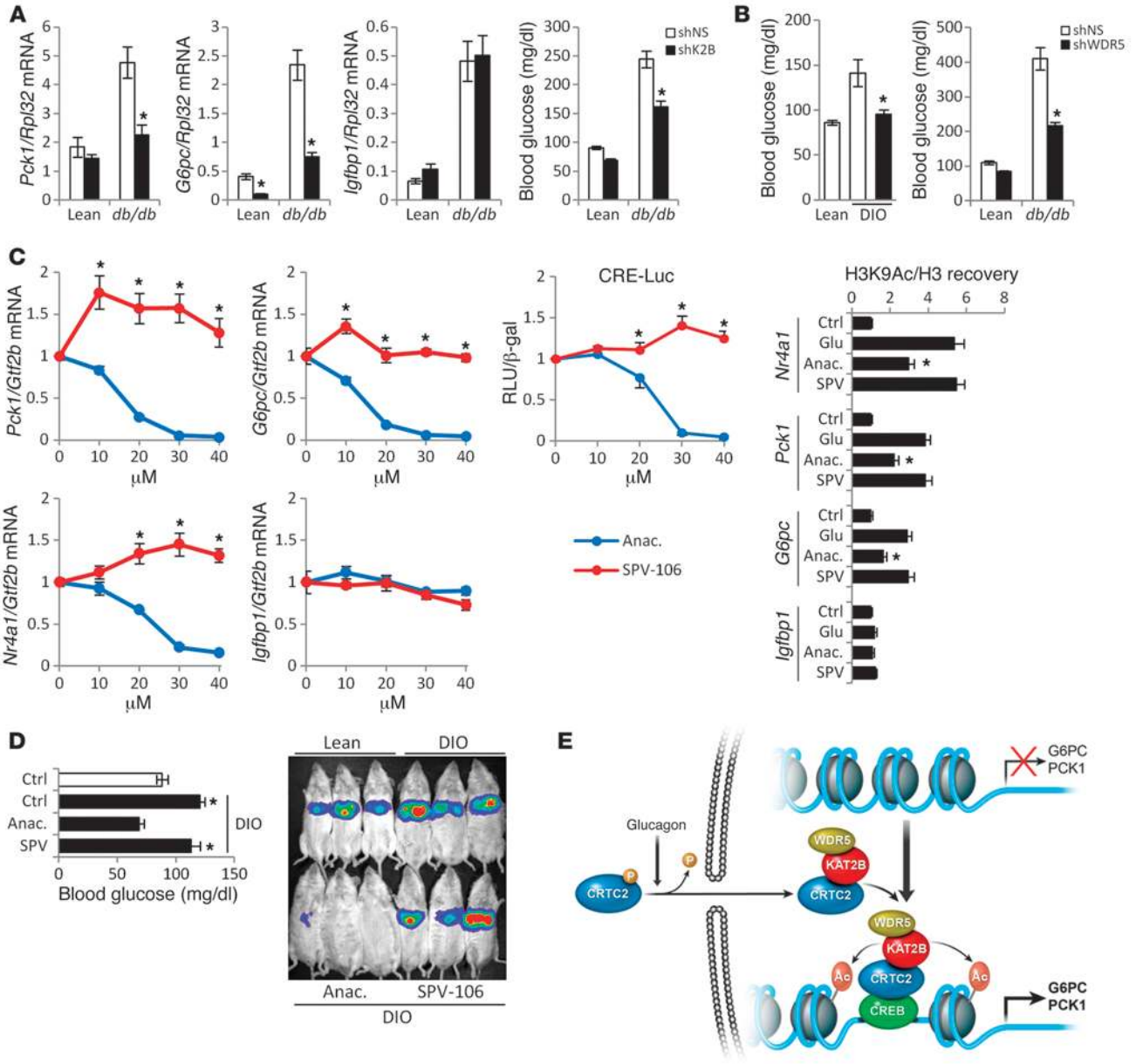

Figure 5

Inhibiting hepatic KAT2B activity lowers blood glucose concentrations in diabetes. (**A**) Effect of hepatic *Kat2b* depletion on gluconeogenic gene expression and blood glucose concentrations in lean *db*/+ and diabetic *db*/*db* mice fasted for 12 hours. (**B**) Effects of acute knockdown of *Wdr5* on fasting blood glucose in livers of 12-hour fasted, lean, HFD-fed (DIO), or diabetic *db*/*db* mice. (**C**) Effect of AA (Anac.) and chemically related derivative SPV-106 on mRNA amounts (left), CRE-Luc activity, and H3K9Ac over gluconeogenic genes (right) in hepatocytes exposed to glucagon (Glu). (**D**) Fasting blood glucose and hepatic CRE-Luc activity in lean and DIO *Cre-Luc* transgenic mice injected i.p. for 5 consecutive days with AA (15 mg/kg), SPV-106, or vehicle. (**E**) Epigenetic regulation of the gluconeogenic program during fasting and in diabetes. Increases in circulating glucagon trigger the dephosphorylation and nuclear translocation of CRTC2, which associates with and mediates the recruitment of KAT2B and WDR5 to CREB binding sites on gluconeogenic promoters. In turn, KAT2B and WDR5 upregulate gluconeogenic genes through a self-reinforcing cycle in which increases in H3K9 acetylation further enhance CREB and CRTC2 occupancy (*$P < 0.05$ relative to lean mice; $n = 4$).

H3K9Ac, which further enhance both CREB and CRTC2 occupancy over gluconeogenic promoters. Breaking this cycle by inhibiting KAT2B activity would be predicted to reverse the attendant hyperglycemia in this setting. Supporting this idea, RNAi-mediated knockdown of hepatic *Kat2b* lowered gluconeogenic gene expression as well as 12-hour fasting blood glucose concentrations in *db*/*db* mice as well as in HFD-fed animals (Figure 5A and Supplemental Figure 9A). Pointing to a specific effect on the CREB pathway, *Kat2b* depletion did not alter mRNA amounts for the fasting-inducible FOXO1 target gene *Igfbp1* (Figure 5A). In keeping with the ability for WDR5 to potentiate KAT2B activity, hepatic depletion of *Wdr5* also reduced blood glucose concentrations in both diet-induced obese (DIO) mice and diabetic *db*/*db* mice (Figure 5B). Taken together, these results indicate that hepatic KAT2A/B and

WDR5 contribute to increases in hepatic glucose production in diabetes through their effects on the CREB/CRTC2 pathway.

If KAT2B stimulates the gluconeogenic program via increases in H3K9Ac, then compounds that inhibit KAT2B acetyltransferase activity may also exhibit glucose-lowering effects. To test this notion, we used anacardic acid (AA), a natural compound with KAT2B inhibitory activity (20, 21). Consistent with its proposed role, exposure to AA reduced H3K9Ac amounts over gluconeogenic genes in hepatocytes treated with glucagon, but a chemically related derivative with no specificity toward KAT2B (SPV-106) (22) did not (Figure 5C). Correspondingly, exposure to AA but not SPV-106 disrupted glucagon-dependent increases in *G6pc*, *Pck1*, and *Nr4a1* mRNA amounts in a dose-dependent manner, having no effect on mRNA amounts for the FOXO target gene *Igfbp1*. In keeping with the apparent selectivity for CREB target genes, exposure to AA also reduced CRE-Luc reporter activity in hepatocytes stimulated with glucagon (Figure 5C).

Similar to its effects in primary hepatocytes, AA administration also reduced H3K9Ac amounts over gluconeogenic genes in lean, fasted C57Bl/6J mice (Supplemental Figure 9F). Correspondingly, we found that AA treatment lowered CRTC2 occupancy and RNA polymerase II recruitment, leading to lower levels of *Pck1* and *G6pc* gene expression and to the downregulation of circulating glucose concentrations (Supplemental Figure 9, D–H). In contrast to its glucose-lowering activity in lean C57Bl/6J mice, AA had no effect on other metabolic parameters including body weight, physical activity, food intake, or respiratory quotient (Supplemental Figure 10, A–C).

To test whether KAT2A and KAT2B mediate hepatic effects of AA, we depleted mice of both enzymes. KAT2A/B depletion downregulated the gluconeogenic program and reduced fasting blood glucose concentrations relative to control mice (Supplemental Figure 9, D and E). In contrast to its effects in control mice, AA did not further downregulate gluconeogenic gene expression or fasting blood glucose levels in KAT2-depleted animals, demonstrating the importance of KAT2A and KAT2B in this setting. We observed a similar requirement for KAT2A/B for AA repression in primary hepatocytes (Supplemental Figure 9C).

Based on the ability of AA to reduce gluconeogenic gene expression in hepatocytes and lean mice, we wondered whether this compound exhibits glucose-lowering effects in the setting of insulin resistance. AA i.p. administration (15 mg/kg) substantially inhibited hepatic CRE-Luc reporter activity in DIO *Cre-Luc* transgenic mice exposed to glucagon, but SPV-106 did not (Figure 5D). As a result, AA, but not SPV-106, administration reduced circulating glucose concentrations in HFD-fed DIO mice and in *db/db* animals (Figure 5D and Supplemental Figure 9B). We observed that circulating insulin levels, body weight, and composition were unaffected by AA (Supplemental Figure 10, D–G). Taken together, these results demonstrate that epigenetic changes over metabolic genes contribute to pathological changes in glucose balance and that small molecules that block these changes may provide therapeutic benefit to diabetic individuals.

Discussion

During fasting, increases in circulating glucagon stimulate hepatic glucose output through induction of the gluconeogenic program. FOXO1 has been shown to transmit the effects of insulin signaling on gluconeogenic gene expression, while CREB and its coactivators appear to mediate the effects of glucagon (3, 23, 24). Depleting CRTC2 in the liver through RNAi-mediated knockdown or targeted disruption of the *Crtc2* gene lowers hepatic glucose production, particularly under HFD conditions, in which the CREB/CRTC2 pathway is constitutively upregulated.

Other regulators appear capable of mediating the effects of glucagon on hepatic gluconeogenesis. In a recent study, knockout of the *Crtc2* gene did not appear to lower fasting blood glucose levels in vivo, even though it disrupted the glucagon-dependent induction of gluconeogenic genes in cultured hepatocytes (25). Pointing to one potential compensatory mechanism, we found that CRTC3 is also activated by glucagon in hepatocytes, where it stimulates gluconeogenic gene expression. Previously characterized by its ability to modulate lipid metabolism in white and brown adipose tissue (26), CRTC3 also appears to regulate the hepatic gluconeogenic program in concert with CRTC2.

In addition to its effects on CRTC2 and CRTC3 activation, glucagon also triggers gluconeogenic gene expression via the phosphorylation of CREB at Ser133 and the recruitment of CBP and P300 to the promoters (27). Although CRTCs and CBP/P300 are thought to act cooperatively in regulating CREB target gene expression, recent work suggests that the individual pathways (CREB/CRTC and CREB/P300/CBP) can function independently (28). In that event, residual glucagon-inducible gene expression in CRTC2-null mice may also reflect the compensatory upregulation of the CREB/P300/CBP pathway. In line with this idea, acute hepatic knockdown of CRTC2 appears to upregulate circulating concentrations of glucagon, evidently by reducing glucagon clearance from the circulation (29). The increase in circulating glucagon could, in principle, compensate for the loss of CRTC2 by further increasing CREB phosphorylation.

Separate from its effects on the CREB/CRTC pathway, glucagon has also been shown to trigger the gluconeogenic program via the induction of class IIa histone deacetylases (HDACs) (30, 31). Sequestered in the cytoplasm under basal conditions, class IIa HDACs (HDAC4, 5, and 7) are dephosphorylated and shuttle to the nucleus in response to glucagon stimulation. Following their entry into the nucleus, class IIa HDACs stimulate the gluconeogenic program by promoting the deacetylation of FOXO1. Future studies should reveal the extent to which this pathway compensates for loss of the CREB/CRTC2 pathway in *Crtc2* mutant mice.

The histone acetylation state is increased over gluconeogenic promoters during fasting and in HFD feeding, consistent with the increases in hepatic glucose production previously reported for these models (4, 32). We found that CRTC2 stimulates gluconeogenic gene expression during fasting and in diabetes primarily by mediating the recruitment of the histone acetyl transferase KAT2B, the predominant KAT2 isoform in the mouse liver. Both KAT2A and KAT2B were found to associate with CRTC2 following its dephosphorylation in response to glucagon. KAT2A/B interact with a conserved C-terminal TAD in CRTC2, and mutations in the TAD that disrupt KAT2A/B binding correspondingly block the induction of gluconeogenic genes. Following their recruitment to the promoter, KAT2A/B were found to enhance gluconeogenic gene expression in part by triggering histone H3K9 acetylation, leading to further increases in CREB and CRTC2 occupancy (Figure 5E). Indeed, the HMT core component WDR5 was also found to modulate gluconeogenic gene expression by potentiating KAT2B activity.

Although they regulate a relatively small subset of genes in hepatocytes, KAT2B and WDR5 are required for the expression of a large fraction of glucagon-inducible genes, indicating that they function importantly as cofactors for the CREB pathway. CRTC2 recruitment represents an early event in cAMP-dependent

promoter activation relative to CREB phosphorylation and CBP/P300 recruitment (33). By increasing H3K9 acetylation over the promoter, KAT2B and WDR5 appear to enhance the accessibility of CREB for PKA-mediated phosphorylation, thereby allowing for the subsequent recruitment of CBP. Supporting this notion, depletion of KAT2B reduced pCREB (Ser133) amounts over CREB binding sites and correspondingly disrupted CBP recruitment in response to cAMP. Indeed, other histone marks that are associated with active transcription also appear to enhance CREB phosphorylation (18), pointing to a more general mechanism by which these modifications may regulate cellular gene expression. Future studies should reveal the extent to which different histone modifications function cooperatively in this setting.

In addition to their direct effects, CREB and CRTC2 have also been found to stimulate the gluconeogenic program indirectly by upregulating the expression of the nuclear hormone receptor coactivator PPAR gamma coactivator 1 (PGC1α). PGC1α activity is further modulated by GCN5/KAT2A, which acetylates and inhibits PGC1α activity by targeting its relocalization to subnuclear structures that also contain the nuclear hormone corepressor RIP140 (34, 35). When fasting is prolonged, PGC1α activity is enhanced through deacetylation by the NAD^+-dependent protein deacetylase SIRT1 (36, 37). Despite these effects on PGC1α activity, SIRT1 overexpression has been found to reduce fasting glucose levels, particularly under HFD feeding conditions, in which the gluconeogenic program is constitutively active. In line with these results, SIRT1 has been found to downregulate the CREB pathway (38, 39) through deacetylation of both CREB and CRTC2.

The discordant effects of KAT2 and SIRT1 on CREB and PGC1α pathways in liver may reflect temporal differences in the activation of these regulators. CREB and CRTC2 have been shown to mediate the acute induction of hepatic gluconeogenesis in response to glucagon, whereas PGC1α activity appears to peak at later times when SIRT1 is maximally activated. Alternatively, CRTC2 and PGC1α may be recruited to distinct cellular target genes that impact the fasting adaptation. Future studies comparing the effects of KAT2 on the recruitment of CRTC2 and PGC1α to gluconeogenic and other metabolic genes in liver should provide insight into this process.

Methods

Animals. Studies with *db/db* mice were performed using 12-week-old male BKS.Cg-*Dock7*$^{m+/+}$*Lepr*^{db}/J mice from The Jackson Laboratory and age-matched *db/+* heterozygous mice as lean controls. All other studies with lean mice were performed using 8- to 10-week-old C57Bl/6J males. *Crtc2*$^{-/-}$, *Kat2b*$^{-/-}$, and *Cre-Luc* mice were described previously (26, 40, 41). *Kat2b* knockout mice were generated by targeting a 5′ exon within the coding region of *Kat2b* (41). The *Kat2b* transcript is prematurely terminated due to insertion of an SV40 polyA sequence and a PGK-neo cassette at this site. *Kat2b*$^{-/-}$ mice were generated by heterozygous intercrosses and appeared phenotypically normal. *Kat2b*$^{-/-}$ mice were used at 12 weeks of age along with age-matched wild-type littermate controls. Body weights for wild-type and *Kat2b* mutant mice were comparable (Supplemental Table 2A). All mice were adapted to their environment for 2 weeks before studies and were housed in colony cages with a 12-hour light/12-hour dark cycle in a temperature-controlled environment. Where indicated as DIO in Figure 5, mice were fed an HFD (60% kcal%, D12492; Research Diets Inc.) or normal chow for 8 weeks. Where indicated in the figures, livers were acutely depleted for specific factors using retroorbital infection with an adenovirus (3×10^9 PFU/kg). Potential liver toxicity following adenoviral injection was monitored by measuring alanine transaminase activities with the Alanine Transaminase Activity Assay Kit from Cayman Chemical (catalog 700260). No mice in this study exhibited liver toxicity. Animal weights were recorded for each experiment and are shown in Supplemental Table 2A.

In vivo analysis. For in vivo imaging, *Cre-Luc* mice were injected with 100 mg/kg glucagon and imaged as described (26). Pyruvate tolerance was tested by i.p. injection of 12-hour fasted mice with 2 g/kg sodium pyruvate followed by blood glucose measurements every 30 minutes over a 2-hour period. Insulin tolerance was tested by i.p. injection of 6-hour fasted mice with 1 U/kg insulin (Humulin R; Eli Lilly) followed by blood glucose measurements every 15 minutes for 1 hour. For determination of blood glucose, serum insulin, glucagon, and alanine transaminase levels, mice were fasted for 12 hours from 8 pm until 8 am. Blood glucose values were determined using a LifeScan automatic glucometer, and serum insulin levels were measured using the Mercodia Ultrasensitive Mouse Insulin ELISA (catalog 10-1249-01). Glucagon levels were determined using the Glucagon Chemiluminescent ELISA kit from Millipore (catalog EZGLU-30K). For measurements of food and water intake, locomotor activity, and respiratory exchange ratio, mice were housed individually in LabMaster (TSE Systems) metabolic cages. Data were collected for 2 to 3 days and analyzed. Body composition was measured using the EchoMRI 100 (Echo Medical Systems LLC).

Hepatic glucose production. Hepatic glucose production was measured as described (42). Briefly, dual catheters were implanted in the jugular vein, tunneled subcutaneously, and exteriorized at the back of the neck. Mice were allowed to recover for 4 days prior to basal hepatic glucose production measurement. After 6 hours of fasting, the experiment began with constant infusion (5 μCi/hour) of D-[3-^{3}H] glucose (DuPont NEN) for 90 minutes. Basal blood sampling was done at 90 minutes and 100 minutes after tracer infusion began. Tracer-determined hepatic glucose production was quantified using the Steele equation (43).

In vitro analysis. HEK293T (ATCC) cells were cultured in DMEM containing 10% FBS (HyClone) and 100 mg/ml penicillin-streptomycin. To generate a stable HEK293T cell line containing the GAL4-Luc cassette, cells were transfected with the GAL4-Luc cassette, and colonies were picked and maintained in neomycin. Primary hepatocytes were derived from C57BL/6J, *Kat2B*$^{-/-}$, or *Crtc2*$^{-/-}$ mice and maintained in serum-free medium 199. Cells were transduced 12 hours after harvesting. Knockdown and overexpression studies in hepatocytes were done by infecting cells at 2 to 5 PFU/cell. All adenoviral shRNA knockdowns were carried out for 60 hours. Where indicated as Glu in Figures 2–4, hepatocytes were stimulated with glucagon (100 nmol/l, G2044; Sigma-Aldrich). Glucose secretion assays were performed as described (40) and were normalized to total protein.

Plasmids and viruses. Recombinant adenoviruses were generated as previously described (44). Specific shRNA sequences are in alphabetical order (alternative sequences are in parentheses): ASH2L: GGGATATGTACAAAATGGTT; ATAC2: GGGATCGCCACATTCATGAT; CBP: GGTGCTGAACATCCTTAAAT; FAM48A: GGGTAGTTAATCAATACCA; KAT2A: GGGCTTCTCCAAAGACATCAA; KAT2B: GGGTTGATTGACAAGTGATT (GGGATTCACAGAGATTGTTT); RBBP5: GGGATGTTCTTTCAGGAGATT; WDR5: GGGCAAGTTCATCTGCTGATA (GGGAAGTGCCTGAAGACATA); YEATS2: GGGACAACAGACACTGAAA; ZZZ3: GGGTTCTGAACGCATGCCAGT.

HAT inhibitors. For in vitro studies, primary hepatocytes were pretreated with either AA (A7236; Sigma-Aldrich) or SPV-106 (SML0154; Sigma-Aldrich) for 30 minutes. For in vivo studies, *Cre-Luc* mice or *db/db* mice were injected i.p. with 15 mg/kg of either compound or vehicle (PBS DMSO, 5:1) for 5 consecutive days.

Antibodies. Antibodies used for immunoblotting and IP are indicated in alphabetical order: ASH2L (A300-112A; Bethyl), CBP antibody A-22 (sc-369; Santa Cruz Biotechnology Inc.), CRTC3 (2720; Cell Signaling Technol-

ogy), FLAG M2 (A8592; Sigma-Aldrich), FOXO1 (2880; CST), pFOXO1 (pS256) (9461; CST), GCN5 (sc-20698; Santa Cruz Biotechnology Inc.), HA clone 3F10 (12013819001; Roche), histone H3 (ab1791; Abcam), H3K27Ac (ab4729; Abcam), H3K27me3 (07-449; Millipore), H3K36me3 (ab9050; Abcam), H3K4me1 (ab8895; Abcam), H3K4me2 (17-677; Millipore), H3K4me3 (17-614; Millipore), H3K9Ac (ab4441; Abcam), KAT2B (3378; CST), RBBP5 (A300-109A; Bethyl), RNA polymerase II (sc-9001; Santa Cruz Biotechnology Inc.), and WDR5 (07-706; Millipore). For CREB, pCREB (pSer133), and CRTC2 detection, rabbit polyclonal antibodies were raised against their respective antigens (5, 45, 46). SPT20 and ZZZ3 antisera were previously described (15). FOXO1 antiserum was provided by Anne Brunet (Stanford University, Stanford, California, USA).

ChIP assays. For analysis of liver chromatin, livers were excised and immediately cross-linked in 1% formaldehyde while being minced with scissors. For preparation of chromatin from primary hepatocytes, cells were cross-linked in 1% formaldehyde directly in the dishes. After 10 minutes of cross-linking, excessive formaldehyde was inactivated with glycine. Nuclei were isolated using a hypotonic lysis buffer and Dounce homogenization, and chromatin was sonicated 8 times for 10 seconds at 50% output. Chromatin was precleared and incubated with the indicated antibodies overnight in the presence of protease, phosphatase, and HDAC inhibitors. Precipitated chromatin was purified, quantified by PCR (Lightcycler 480; Roche), and presented as a percentage of input chromatin. For modified histone ChIPs, chromatin was precipitated with antibodies detecting the specific histone modification as well as total histone H3; these were subjected to relative quantification by quantitative PCR using standard curves for each primer set. Quantified levels of chromatin precipitated by modification-specific histone H3 antibodies are shown as a fraction of quantified chromatin precipitated by the nondiscriminating histone H3 antibody. Primer sequences are listed in Supplemental Table 1.

Gene expression. Total cellular RNA from whole liver or from primary hepatocytes was extracted using the RNeasy kit (QIAGEN), and cDNA was generated using the iScript select system (Bio-Rad). cDNA was quantified on a Lightcycler 480 instrument (Roche). Gene expression data were presented relative to the expression of housekeeping genes *Gtf2b* (hepatocytes) and *Rpl32* (liver). Primer sequences are listed in Supplemental Table 1. For global analysis of gene expression, hepatocytes were depleted of either *Wdr5* or *Kat2b* and stimulated with glucagon (100 nM) for 90 minutes. Control hepatocytes were transduced with nonspecific (NS) shRNA and treated with glucagon or left untreated. Total RNA was converted to cDNA and hybridized to GeneChip Mouse Gene 1.0 ST Arrays (Affymetrix). Arrays were normalized and analyzed using Affymetrix Expression Console v. 1.1 software, and data are available through the Gene Expression Omnibus database (GEO GSE47179). GO analysis was performed using GOrilla (http://cbl-gorilla.cs.technion.ac.il).

Protein analysis. Total protein from whole liver or primary hepatocytes was extracted in a Tris-HCl buffer containing 1% NP40 and protease and phosphatase inhibitors. Proteins were quantified using BCA reagents (Pierce) and separated using SDS-PAGE. For pulldown experiments, GST proteins were all bacterially expressed and purified. Full-length WDR5 and KAT2B were expressed in HEK293T cells as Halo-tagged (Promega) fusion proteins, purified to homogeneity and cleaved from the Halo tag using the TEV protease (V6051; Promega).

Statistics. All studies were performed on at least three independent occasions. Results are reported as the mean ± SD. The comparison of different groups was carried out using a two-tailed, unpaired Student's *t* test and two-way ANOVA. Differences were considered statistically significant at $P < 0.05$. Hypergeometric distribution of microarray data was calculated by comparing glucagon-induced genes as a fraction of either all expressed genes or genes reduced by *Kat2b* depletion.

Study approval. All animal procedures were performed with a protocol approved by the IACUC of the Salk Institute for Biological Studies.

Acknowledgments

This work was supported by NIH grants R01-DK049777, R01-DK083834, R01-DK091618, P30-DK063491, P01-DK074868, and R01-DK33651. Support was also provided by the Clayton Foundation for Medical Research, the Kieckhefer Foundation, the Leona M. and Harry B. Helmsley Charitable Trust, and the Danish Research Council. We thank David Allis (The Rockefeller University) and Joanna Wysocka (Stanford University) for the WDR5 reagents and Anne Brunet (Stanford University) for the FOXO1 antiserum.

Received for publication January 28, 2013, and accepted in revised form July 24, 2013.

Address correspondence to: Marc Montminy, The Salk Institute, 10010 N. Torrey Pines Rd., La Jolla, California 92037, USA. Phone: 858.453.4100; Fax: 858.552.1546; E-mail: montminy@salk.edu.

1. Lu M, et al. Insulin regulates liver metabolism in vivo in the absence of hepatic Akt and Foxo1. *Nat Med*. 2012;18(3):388–395.
2. Herzig S, et al. CREB regulates hepatic gluconeogenesis through the coactivator PGC-1. *Nature*. 2001;413(6852):179–183.
3. Koo SH, et al. The CREB coactivator TORC2 is a key regulator of fasting glucose metabolism. *Nature*. 2005;437(7062):1109–1111.
4. Saberi M, et al. Novel liver-specific TORC2 siRNA corrects hyperglycemia in rodent models of type 2 diabetes. *Am J Physiol Endocrinol Metab*. 2009; 297(5):E1137–E1146.
5. Screaton RA, et al. The CREB coactivator TORC2 functions as a calcium- and cAMP-sensitive coincidence detector. *Cell*. 2004;119(1):61–74.
6. Dentin R, et al. Insulin modulates gluconeogenesis by inhibition of the coactivator TORC2. *Nature*. 2007;449(7160):366–369.
7. Wang Y, et al. Inositol-1,4,5-trisphosphate receptor regulates hepatic gluconeogenesis in fasting and diabetes. *Nature*. 2012;485(7396):128–132.
8. Jin Q, et al. Distinct roles of GCN5/PCAF-mediated H3K9ac and CBP/p300-mediated H3K18/27ac in nuclear receptor transactivation. *EMBO J*. 2011; 30(2):249–262.
9. Nagy Z, et al. The metazoan ATAC and SAGA coactivator HAT complexes regulate different sets of inducible target genes. *Cell Mol Life Sci*. 2010; 67(4):611–628.
10. Wysocka J, et al. WDR5 associates with histone H3 methylated at K4 and is essential for H3 K4 methylation and vertebrate development. *Cell*. 2005;121(6):859–872.
11. Yamauchi T, et al. Distinct but overlapping roles of histone acetylase PCAF and of the closely related PCAF-B/GCN5 in mouse embryogenesis. *Proc Natl Acad Sci U S A*. 2000;97(21):11303–11306.
12. Clements A, Rojas JR, Trievel RC, Wang L, Berger SL, Marmorstein R. Crystal structure of the histone acetyltransferase domain of the human PCAF transcriptional regulator bound to coenzyme A. *EMBO J*. 1999;18(13):3521–3532.
13. Grant PA, et al. Yeast Gcn5 functions in two multisubunit complexes to acetylate nucleosomal histones: characterization of an Ada complex and the SAGA (Spt/Ada) complex. *Genes Dev*. 1997; 11(13):1640–1650.
14. Ogryzko VV, et al. Histone-like TAFs within the PCAF histone acetylase complex. *Cell*. 1998;94(1):35–44.
15. Krebs AR, Karmodiya K, Lindahl-Allen M, Struhl K, Tora L. SAGA and ATAC histone acetyl transferase complexes regulate distinct sets of genes and ATAC defines a class of p300-independent enhancers. *Mol Cell*. 2011;44(3):410–423.
16. Wang YL, Faiola F, Xu M, Pan S, Martinez E. Human ATAC Is a GCN5/PCAF-containing acetylase complex with a novel NC2-like histone fold module that interacts with the TATA-binding protein. *J Biol Chem*. 2008;283(49):33808–33815.
17. Guelman S, et al. Host cell factor and an uncharacterized SANT domain protein are stable components of ATAC, a novel dAda2A/dGcn5-containing histone acetyltransferase complex in Drosophila. *Mol Cell Biol*. 2006;26(3):871–882.
18. Tsai WW, Niessen S, Goebel N, Yates JR, Guccione E, Montminy M. PRMT5 modulates the metabolic response to fasting signals. *Proc Natl Acad Sci U S A*. 2013;110(22):8870–8875.
19. Conkright MD, et al. TORCs: transducers of regulated CREB activity. *Mol Cell*. 2003;12(2):413–423.
20. Balasubramanyam K, Swaminathan V, Ranganathan A, Kundu TK. Small molecule modulators of histone acetyltransferase p300. *J Biol Chem*. 2003;278(21):19134–19140.

21. Ghizzoni M, Boltjes A, Graaf C, Haisma HJ, Dekker FJ. Improved inhibition of the histone acetyltransferase PCAF by an anacardic acid derivative. *Bioorg Med Chem*. 2010;18(16):5826–5834.
22. Sbardella G, et al. Identification of long chain alkylidenemalonates as novel small molecule modulators of histone acetyltransferases. *Bioorg Med Chem Lett*. 2008;18(9):2788–2792.
23. Matsumoto M, Pocai A, Rossetti L, Depinho RA, Accili D. Impaired regulation of hepatic glucose production in mice lacking the forkhead transcription factor foxo1 in liver. *Cell Metab*. 2007;6(3):208–216.
24. Haeusler RA, Kaestner KH, Accili D. FoxOs function synergistically to promote glucose production. *J Biol Chem*. 2010;285(46):35245–35248.
25. Le Lay J, Tuteja G, White P, Dhir R, Ahima R, Kaestner KH. CRTC2 (TORC2) contributes to the transcriptional response to fasting in the liver but is not required for the maintenance of glucose homeostasis. *Cell Metab*. 2009;10(1):55–62.
26. Song Y, et al. CRTC3 Links catecholamine signaling to energy balance. *Nature*. 2010;468(7326):933–939.
27. Altarejos JY, Montminy M. CREB and the CRTC co-activators: sensors for hormonal and metabolic signals. *Nat Rev Mol Cell Biol*. 2011;12(3):141–151.
28. Xu W, Kasper LH, Lerach S, Jeevan T, Brindle PK. Individual CREB-target genes dictate usage of distinct cAMP-responsive coactivation mechanisms. *EMBO J*. 2007;26(12):2890–2903.
29. Erion DM, et al. CREB-regulated transcription coactivator 2 (CRTC2) promotes glucagon clearance and hepatic amino acid catabolism to regulate glucose homeostasis. *J Biol Chem*. 2013;288(22):16167–16176.
30. Mihaylova MM, et al. Class IIa histone deacetylases are hormone-activated regulators of FOXO and mammalian glucose homeostasis. *Cell*. 2011; 145(4):607–621.
31. Wang B, et al. A hormone-dependent module regulating energy balance. *Cell*. 2011;145(4):596–606.
32. Samuel VT, et al. Targeting foxo1 in mice using antisense oligonucleotide improves hepatic and peripheral insulin action. *Diabetes*. 2006;55(7):2042–2050.
33. Ravnskjaer K, et al. Cooperative interactions between CBP and TORC2 confer selectivity to CREB target gene expression. *EMBO J*. 2007;26(12):2880–2889.
34. Dominy JE Jr, et al. The deacetylase Sirt6 activates the acetyltransferase GCN5 and suppresses hepatic gluconeogenesis. *Mol Cell*. 2012;48(6):900–913.
35. Dominy JE, Lee Y, Gerhart-Hines Z, Puigserver P. Nutrient-dependent regulation of PGC-1α's acetylation state and metabolic function through the enzymatic activities of Sirt1/GCN5. *Biochim Biophys Acta*. 2010;1804(8):1676–1683.
36. Rodgers JT, Lerin C, Haas W, Gygi SP, Spiegelman BM, Puigserver P. Nutrient control of glucose homeostasis through a complex of PGC-1α and SIRT1. *Nature*. 2005;434(7029):113–118.
37. Erion DM, et al. SirT1 knockdown in liver decreases basal hepatic glucose production and increases hepatic insulin responsiveness in diabetic rats. *Proc Natl Acad Sci U S A*. 2009;106(27):11288–11293.
38. Qiang L, Lin HV, Kim-Muller JY, Welch CL, Gu W, Accili D. Proatherogenic abnormalities of lipid metabolism in SirT1 transgenic mice are mediated through Creb deacetylation. *Cell Metab*. 2011; 14(6):758–767.
39. Liu Y, et al. A fasting inducible switch modulates gluconeogenesis via activator/coactivator exchange. *Nature*. 2008;456(7219):269–273.
40. Wang Y, et al. Targeted disruption of the CREB coactivator Crtc2 increases insulin sensitivity. *Proc Natl Acad Sci U S A*. 2010;107(7):3087–3092.
41. Xu W, Edmondson DG, Evrard YA, Wakamiya M, Behringer RR, Roth SY. Loss of Gcn5l2 leads to increased apoptosis and mesodermal defects during mouse development. *Nat Genet*. 2000;26(2):229–232.
42. Li P, et al. Adipocyte NCoR knockout decreases PPARgamma phosphorylation and enhances PPARgamma activity and insulin sensitivity. *Cell*. 2011;147(4):815–826.
43. Steele R. Influences of glucose loading and of injected insulin on hepatic glucose output. *Ann N Y Acad Sci*. 1959;82:420–430.
44. Du K, Herzig S, Kulkarni RN, Montminy M. TRB3: a tribbles homolog that inhibits Akt/PKB activation by insulin in liver. *Science*. 2003; 300(5625):1574–1577.
45. Gonzalez GA, Menzel P, Leonard J, Fischer WH, Montminy MR. Characterization of motifs which are critical for activity of the cyclic AMP-responsive transcription factor CREB. *Mol Cell Biol*. 1991; 11(3):1306–1312.
46. Hagiwara M, et al. Coupling of hormonal stimulation and transcription via cyclic AMP-responsive factor CREB is rate limited by nuclear entry of protein kinase A. *Mol Cell Biol*. 1993;13(8):4852–4859.